



**HAL**  
open science

## Electric field control of electromagnon frequency in multiferroics

S. Omid Sayedaghaee, Charles Paillard, Sergey Prosandeev, Sergei Prokhorenko, Yousra Nahas, Bin Xu, L. Bellaïche

► **To cite this version:**

S. Omid Sayedaghaee, Charles Paillard, Sergey Prosandeev, Sergei Prokhorenko, Yousra Nahas, et al.. Electric field control of electromagnon frequency in multiferroics. *Physical Review Materials*, 2022, 6 (12), pp.124404. 10.1103/PhysRevMaterials.6.124404 . hal-03899769

**HAL Id: hal-03899769**

**<https://hal-centralesupelec.archives-ouvertes.fr/hal-03899769>**

Submitted on 15 Dec 2022

**HAL** is a multi-disciplinary open access archive for the deposit and dissemination of scientific research documents, whether they are published or not. The documents may come from teaching and research institutions in France or abroad, or from public or private research centers.

L'archive ouverte pluridisciplinaire **HAL**, est destinée au dépôt et à la diffusion de documents scientifiques de niveau recherche, publiés ou non, émanant des établissements d'enseignement et de recherche français ou étrangers, des laboratoires publics ou privés.

1 **Electric-field-control of electromagnons' frequency in multiferroics**

2 S. Omid Sayedaghaee,<sup>1</sup> Charles Paillard,<sup>2</sup> Sergey Prosandeev,<sup>1</sup>  
3 Sergei Prokhorenko,<sup>1</sup> Yousra Nahas,<sup>1</sup> Bin Xu,<sup>3</sup> and L. Bellaiche<sup>1</sup>

4 <sup>1</sup>*Physics Department and Institute for Nanoscience and Engineering,*  
5 *University of Arkansas, Fayetteville, Arkansas 72701, USA*

6 <sup>2</sup>*Laboratoire Structures, Propriétés et Modélisation des Solides,*  
7 *CentraleSupélec, CNRS UMR 8580,*  
8 *Université Paris-Saclay, 91190 Gif-sur-Yvette, France*

9 <sup>3</sup>*Institute of Theoretical and Applied Physics*  
10 *and School of Physical Science and Technology,*  
11 *Soochow University, Suzhou, Jiangsu 215006, China*

12 (Dated: October 25, 2022)

# Abstract

13

14 Electromagnons, which are coupled polar and magnetic excitations in magnetoelectric materials,  
15 are of large interest for electronic and computing technological devices. Using Molecular Dynamics  
16 simulations based on an *ab-initio* effective Hamiltonian, we predict that the frequency of several  
17 electromagnons can be tuned by the application of electric fields in the model multiferroic BiFeO<sub>3</sub>,  
18 with this frequency either increasing or decreasing depending on the selected electromagnon. In  
19 particular, we show that the frequency of electromagnons localized at ferroelectric domain walls can  
20 be tuned over a 200 GHz range by realistic dc electric fields. We interpret the realized frequency  
21 increase (respectively, decrease) by local hardening (respectively, softening) of the associated polar  
22 phonons which couples to the applied electric field. The increase *versus* decrease of the elec-  
23 tromagnons' frequency is further found to be correlated with the real-space localization of such  
24 phonons.

## 25 I. INTRODUCTION

26 Electromagnons, a coupled oscillation wave of electrical and magnetic dipoles in magneto-  
27 electric materials, have bolstered large interest since they were first discussed in 1970s [1, 2].  
28 They have remained elusive for a long time, except in a few materials such as rare-earth  
29 (R) manganites RMnO<sub>3</sub> [3–5], RMn<sub>2</sub>O<sub>5</sub> [6, 7] or ferrite perovskite oxides [8–11]. Among  
30 them, BiFeO<sub>3</sub>, a room temperature multiferroic [12], has been one of the most intensely  
31 considered magnetoelectrics for electromagnon detection, characterization and technological  
32 applications. Among the various experimental and theoretical studies of electromagnons,  
33 most have focused on so-called electro-active magnons, *i.e.*, control of spin waves by electric  
34 fields [13–17]. On the other hand, much less work has been devoted to the study of magnetic  
35 control of polarization waves, with a few theoretical works realized in BiFeO<sub>3</sub> [18–20] and  
36 manganites [21]. The present work goes one step further by bridging the two approaches, as  
37 we intend to demonstrate the possibility of resonantly exciting electromagnons (induced by  
38 ferroelectric domain walls) using ac magnetic fields while concurrently manipulating their  
39 frequency with dc electric fields.

40 Note that ferroelectric domain walls can now routinely be written, erased and reconfigured  
41 using, for instance, PiezoForce Microscopy [22–25]. The ability to generate magnetically  
42 polarization waves localized at domain walls, as proposed in Ref. [18], already promises the

43 tantalizing possibility of reconfigurable nanometer size electrical circuits, whose power is  
44 switched on and sustained remotely by ac magnetic fields. If now one is able to act on the  
45 electrical polarized waves localized at the ferroelectric domain walls, for instance using local  
46 electric fields, one could dream of achieving reconfigurable logical elements for computing  
47 or detection.

48 In this work, we investigate how dc electric fields affect the domain-wall-induced electro-  
49 magnons evidenced in Ref. [18] in multiferroic BiFeO<sub>3</sub>. Using Molecular Dynamics based on  
50 an *ab-initio* effective Hamiltonian, we reveal that the frequency of these electromagnons is  
51 rather sensitive to these dc fields, either increasing or decreasing with them depending on  
52 the chosen electromagnon. This latter different behavior (namely, increase *versus* decrease)  
53 is found to be correlated with the real-space localization of the optical phonon associated  
54 with these electromagnons.

## 55 II. METHODS

56 Here and as shown in Figure 1, we simulate a multidomain system of BFO with 180°  
57 domain configuration inside which two types of domains alternate along the [110] pseudo-  
58 cubic direction. The first type of domain, denoted as  $D1$ , is shown in red in Fig. 1 and  
59 possesses electric dipoles aligned along the  $[\bar{1}11]$  direction. The second kind of domain,  
60 coined  $D2$ , is displayed in blue in this figure and exhibits electric dipoles lying along the  
61 opposite  $[1\bar{1}\bar{1}]$  direction. In both domains the magnetic moments and antiferromagnetic  
62 (AFM) moments are along the perpendicular  $[211]$  and  $[0\bar{1}1]$  directions, respectively.

63 The energetics and properties of the studied system are modeled via the use the effective  
64 Hamiltonian framework detailed in Ref. [26] within a molecular dynamics (MD) approach  
65 [27], in order to obtain dynamical properties. Technically, Newtonian equations of motion  
66 are used to investigate the dynamics of the ionic degrees of freedom of this effective Hamil-  
67 tonian – that are local modes which are directly proportional to local electric dipoles inside  
68 each 5-atom cell; pseudo-vectors representing the antiferrodistortive motions inside such 5-  
69 atom cells; and both homogeneous and inhomogeneous strain components. Regarding the  
70 dynamics of the magnetic moments, the approach of Ref. [28] is followed, for which such  
71 dynamics are treated through the Landau-Lifshitz-Gilbert (LLG) equation [29].

72 DC electric fields with magnitude ranging between  $1.0 \times 10^7$  V/m and  $1.0 \times 10^8$  V/m

73 are applied along the  $[\bar{1}11]$  direction to such multidomain, that is currently mimicked by  
 74 using a  $24 \times 24 \times 6$  supercell. It should be noted that an electric field of the magnitude of  
 75  $2.0 \times 10^8$  V/m is strong enough to reorient all dipole moments along its direction and convert  
 76 the configuration to monodomain. The MD simulations are conducted at the temperature of  
 77  $10$  K. To ensure that the magnetic moments only slightly fluctuate about the same direction  
 78 during the course of simulations, a dc magnetic field of the magnitude of  $245$  T is applied  
 79 along the  $[211]$  direction. A lower magnetic field (which is accessible in practical applications)  
 80 could be applied. In fact, we also performed simulations with a *dc* magnetic field having  
 81 a magnitude of  $2.45$  T along the  $[211]$  direction, and obtained similar results. Such a large  
 82 magnetic field along with low temperature were chosen here to avoid large fluctuations of  
 83 magnetic properties and see the results more clearly. Each MD simulation was performed  
 84 for 1,000,000 steps of  $0.5$  fs each, while both homogeneous and inhomogeneous strains were  
 85 relaxed.

### 86 III. RESULTS AND DISCUSSION

87 It is important to realize that, under zero dc electric field, there is no macroscopic polar-  
 88 ization, as a result of the cancellations between the polarizations of the  $D1$  and  $D2$  domains.  
 89 On the other hand, we numerically found that the application of our considered dc electric  
 90 fields results in the increase of the magnitude of electric dipoles in the  $D1$  regions and its  
 91 reduction in the  $D2$  areas, therefore yielding now a finite overall polarization along the direc-  
 92 tion of the applied field which is  $[\bar{1}11]$ . It is worth mentioning that we observed the change  
 93 in the structure from a 180-degree multidomain to a monodomain when the applied electric  
 94 field exceeds a threshold ( $E_{threshold} = 2 \times 10^8$  V/m) which is rather abrupt - at least with  
 95 the resolution of the applied electric field change here, being  $E = 1 \times 10^7$  V/m. One may  
 96 thus need a much smaller step in field's magnitude to observe motion of the domain walls.  
 97 One can also increase the temperature to see such motion. For instance, and as shown in  
 98 the Supplementary Material, motion of the domain walls does occur at  $T = 300$  K when the  
 99 applied electric field varies from  $E = 3 \times 10^7$  V/m to  $E = 5 \times 10^7$  V/m.

100 We then perform Fourier analysis of the temporal evolution of this resulting electrical  
 101 polarization along the  $[\bar{1}11]$  direction, and that of the magnetization along the  $[211]$  direction.  
 102 Figure 2 shows the resulting Fast Fourier Transformations (FFT) of both the electrical

103 polarization and magnetization for a dc electric field of  $1.0 \times 10^7$  V/m, which reveals the  
 104 existence of frequency modes presenting phonons and magnons. Here, in particular, some  
 105 peaks are observed at the same frequency in the FFT spectrum of both polarization and  
 106 magnetization, which is a signature of electromagnons. Within the electromagnonic modes  
 107 that are observed here, four modes are of particular interest due to their noticeable frequency  
 108 shift as a response to the application of electric fields of various magnitudes. These modes  
 109 are denoted by Mode 1, Mode 2, Mode 3, and Mode 4 in Figure 2 (Note that these four  
 110 modes have very similar frequencies than those one can guess to be around  $90 \text{ cm}^{-1}$  ( $\simeq$   
 111  $2700 \text{ GHz}$ ) and  $140 \text{ cm}^{-1}$  ( $\simeq 4200 \text{ GHz}$ ) in the Supplemental materials of Ref. [30] for  
 112 precisely  $180^\circ$  domains of BFO). The electric-field-induced frequency shift of both the phonon  
 113 and magnon associated with the electromagnonic Mode 1 is demonstrated in Figs. 3a and  
 114 3b, respectively. For this mode, as indicated by purple solid lines in Figs. 3a and 3b,  
 115 when the applied electric field is  $1.0 \times 10^7$  V/m the phonon peak is at  $2490 \text{ GHz}$  (Figure  
 116 3a) and the magnon peak is exactly at the same frequency location (Figure 3b). When  
 117 the applied electric field increases to higher magnitudes, the frequency of the phonon and  
 118 magnon decrease concurrently which results in a softening for Mode 1. It should be noted  
 119 that, in multiferroics, strain can contribute to the emergence of so-called electroacoustic  
 120 magnons as a mixture of acoustic phonons, optical phonons, and magnons [19, 20]. Here,  
 121 we numerically found (not shown here) that the four aforementioned modes are present in  
 122 the frequency spectrum of both the polarization and magnetization even if the homogeneous  
 123 strain is clamped during the course of MD simulations, which clarifies that these modes are  
 124 electromagnons consisting of optical phonons and magnons. *It should be noted that we*  
 125 *do not believe that these computed intensities of Figure 3 have a real physical meaning in*  
 126 *our simulations, since such intensities are not monotonic with the fields and can vary when*  
 127 *slightly changing some technical details of the Fourier Transform (especially, considering the*  
 128 *small values of the vertical scale in the Figure). On the other hand, the frequency position*  
 129 *of these peaks is insensitive to such details and does carry physical significance.*

130 For each of these four considered modes, the evolution of their frequency as a function  
 131 of the magnitude of the *dc* electric field is shown in Figure 4. One can see that Mode  
 132 1 experiences a rather strong decrease of its frequency when the electric field varies from  
 133  $1.0 \times 10^7$  V/m to  $1.0 \times 10^8$  V/m, namely by about  $200 \text{ GHz}$  from  $2490 \text{ GHz}$  to  $2290 \text{ GHz}$ .  
 134 Note that it is known that the effective Hamiltonians of BFO overestimate the magnitude

135 of electric fields by a factor of 23 [31]. Hence, our maximum applied electric field would  
 136 correspond experimentally to approximately 43 kV/cm, which is easily sustained in BiFeO<sub>3</sub>  
 137 thin films [32]. Note also that the decrease of the Mode 1 frequency appears to be quadratic  
 138 in nature. Mode 2 also adopts a reduction of its frequency, but at a smaller extent (that  
 139 is by about 55 GHz from 2715 GHz to 2660 GHz) and in a linear fashion, with a rate of  
 140 0.06 GHz/(kV/cm). Interestingly, such linear variation has indeed been observed in BiFeO<sub>3</sub>  
 141 for some electromagnons. For instance, the frequency of the so-called extra-cyclon mode  $\psi_2$   
 142 may increase or decrease (depending on whether the electric field increases or decreases the  
 143 polarization) with a rate of approximately 1.3 GHz/(kV/cm) [33]. In the same reference,  
 144 the cyclon mode  $\phi_2$  shows an opposite behavior with an electrical rate of control of the  
 145 magnon frequency of  $\approx 0.24$  GHz/(kV/cm). Note that we focus here on domain-wall-  
 146 induced electromagnons with an antiferromagnetic structure, while the cyclon and extra-  
 147 cyclon modes considered in Ref [33] are modes in a monodomain single crystal having a  
 148 magnetic cycloidal state. In addition, the commonly known overestimation of electric fields  
 149 in effective Hamiltonian models may also contribute to the difference between computational  
 150 and experimental rates for the dc-field-induced change in frequency. As a matter of fact,  
 151 rescaling our theoretical fields by dividing them by 23 (as indicated in Ref. [31]) results in  
 152 a rate for our Mode 2 that goes from 0.06 GHz/(kV/cm) to 1.38 GHz/(kV/cm), which is  
 153 similar to the observed magnitude of such rate for the  $\psi_2$  mode in Ref [33]. Similarly, Mode  
 154 3 has the same kind of qualitative behavior than Mode 2 but with about twice the slope –  
 155 that is, a linear decrease of its frequency by  $\simeq 117$  GHz when the *dc* electric field strengthens  
 156 from  $1.0 \times 10^7$  V/m to  $1.0 \times 10^8$  V/m. Strikingly, Mode 4, whose frequency is basically that  
 157 of Mode 3 for an interpolated zero field, adopts a mirror behavior with respect to Mode  
 158 3, in the sense that its frequency concomitantly linearly increases by a similar amount of  
 159  $\simeq 117$  GHz. Note that we also performed simulations with *opposite dc* electric fields (i.e.,  
 160 along  $[1\bar{1}\bar{1}]$ ), which allows us to further determine that the frequencies of Modes 1 and 2  
 161 depend on the *magnitude* of the electric field along  $[\bar{1}11]$  or  $[1\bar{1}\bar{1}]$  while those of Modes 3 and  
 162 4 linearly depend on the *projection* of the electric field along  $[\bar{1}11]$  (i.e., on the magnitude  
 163 but also sign of this projection).

164 In order to understand all these behaviors and demonstrate their relationship with real-  
 165 space localization, a layer-by-layer analysis is performed at the different planes that are  
 166 parallel to the domain wall. More precisely, the Fourier transform of the average of po-

167 larization of each of these planes is computed for the frequencies associated with the four  
 168 aforementioned modes for a dc field of  $1.0 \times 10^7$  V/m, and is shown in Figure 5. For instance,  
 169 Panel (a) of Figure 5 tells us that Mode 1 is a mode that is strongly localized at the domain  
 170 walls. Furthermore, Panel (b) of Figure 5 reveals that Mode 2 also localizes near the domain  
 171 walls but to a smaller extent, as seen by comparing its vertical scale with that of Figure  
 172 5(a). Consequently, by looking at Figs 4(a), 4(b), 5(a) and 5(b), one can conclude that  
 173 modes localizing near the domain walls soften under a *dc* electric field, that is they have  
 174 their frequency decreasing when the field increases – and such decrease is larger when the  
 175 localization near the walls is stronger.

176 Interestingly, Figures 5(c) and 5(d) tell us that Modes 3 and 4 are rather different from  
 177 Modes 1 and 2, in the sense that they prefer to localize inside the domains rather than at  
 178 the domain walls. More precisely, Mode 3 reaches its maximum of the Fourier transform  
 179 of the polarization in the *D2* region inside which the polarization is antiparallel to the  
 180 applied electric field. Consequently, applying such field will decrease the magnitude of the  
 181 polarization in the *D2* area, which corresponds to a local softening of the optical phonon,  
 182 hence explaining the decrease of the frequency seen in Fig. 4c for Mode 3. In contrast,  
 183 Mode 4 preferentially localizes in the *D1* area for which the polarization is parallel to the  
 184 *dc* electric field, and, as a result, such polarization increases in magnitude when the field  
 185 strengthens. Such increase leads to a local hardening of Mode 4, therefore to a frequency  
 186 that now increases with the field. Note that Modes 3 and 4 (whose frequency are about  
 187 4210 GHz and 4245 GHz for a field of  $1.0 \times 10^7$  V/m, which correspond to  $140 \text{ cm}^{-1}$  and  
 188  $142 \text{ cm}^{-1}$ , respectively) can be thought as both originating from the known zone-center optical  
 189 phonon of BiFeO<sub>3</sub> monodomain, that then splits in two under dc electric fields because of the  
 190 existence of domain walls and two different types of domains in our studied system. Based  
 191 on previous works on BiFeO<sub>3</sub> monodomain single crystals and the fact that we numerically  
 192 further found (not show here) that Modes 3 and 4 have rather small FFT of the component  
 193 of the polarization along the [110]-direction (which is perpendicular to the polarizations of  
 194 both D1 and D2), one can suggest that Modes 3 and 4 originate from the  $A_1(LO)$  mode,  
 195 rather than the  $E(TO)$  mode, of BiFeO<sub>3</sub> monodomain [28, 34–37].



## 196 IV. SUMMARY

197 In summary, we used an atomistic effective Hamiltonian to reveal that the frequency of  
198 electromagnons can be significantly tuned by applying dc electric fields in the prototypi-  
199 cal  $\text{BiFeO}_3$  multiferroic adopting ferroelectric domains. Such finding is promising towards  
200 the design of novel devices taking advantage of the dual electric and magnetic natures of  
201 electromagnons, with the additional conveniences demonstrated here that (1) it should thus  
202 be possible to select the desired operating frequency by choosing the right combination of  
203 ac magnetic field's frequency and magnitude of the dc electric field (in order to activate  
204 such electromagnons at this desired frequency); and (2) some of these electromagnons are  
205 localized at the ferroelectric domain walls, therefore rendering feasible the application of  
206 local electric fields for realizing reconfigurable logical elements for computing or detection.  
207 These domain-wall-induced electromagnons are further found to either increase or decrease  
208 their frequencies under the dc electric fields, depending on the real-space localization of  
209 their associated phonons— that is at the ferroelectric domain walls or at the “up” *versus*  
210 “down” domains. We therefore hope that the present study deepens the fascinating fields  
211 of electromagnons, ferroelectric domains and magnonics.

## 212 ACKNOWLEDGEMENTS

213 The authors thank the Vannevar Bush Faculty Fellowship (VBFF) Grant No. N00014-20-  
214 1-2834 from the Department of Defense and the ARO Grant No. W911NF-21-1-0113. C.P.  
215 thanks the ANR Grant No. ANR-21-CE24-0032 SUPERSPIN, and a public grant overseen  
216 by the ANR as part of the Investissements d’Avenir program (Reference: ANR-10-LABX-  
217 0035, Labex-NanoSaclay). S.P. also acknowledges ONR Grant No. N00014-21-1-2086. B.X.  
218 further acknowledges the financial support from National Natural Science Foundation of  
219 China under Grant No. 12074277, the startup fund from Soochow University, and the  
220 support from Priority Academic Program Development (PAPD) of Jiangsu Higher Education  
221 Institutions. S.P. and Y.N. thank DARPA Grant No. HR0011727183- D18AP00010 (under  
222 the TEE Program). The authors also acknowledge the High Performance Computing Center

223 at the University of Arkansas and thank Jorge Íñiguez for useful discussions.

---

- 224 [1] Baryakhtar, V. & Chupis, I. Quantum Theory of Oscillations In A Ferroelectric Ferromagnet.  
225 *Soviet Physics Solid State, USSR.* **11**, 2628+ (1970)
- 226 [2] Smolenskii, G. & Chupis, I. Ferroelectromagnets. *Soviet*  
227 *Physics Uspekhi.* **25**, 475-493 (1982), [http://stacks.iop.org/0038-](http://stacks.iop.org/0038-5670/25/i=7/a=R02?key=crossref.14140c0267d9f2ea3f559dade150f3df)  
228 [5670/25/i=7/a=R02?key=crossref.14140c0267d9f2ea3f559dade150f3df](http://stacks.iop.org/0038-5670/25/i=7/a=R02?key=crossref.14140c0267d9f2ea3f559dade150f3df)
- 229 [3] Pimenov, A., Rudolf, T., Mayr, F., Loidl, A., Mukhin, A. & Balbashov, A. Cou-  
230 pling of phonons and electromagnons in GdMnO<sub>3</sub>. *Physical Review B.* **74**, 100403 (2006),  
231 <https://link.aps.org/doi/10.1103/PhysRevB.74.100403>
- 232 [4] Pimenov, A., Mukhin, A., Ivanov, V., Travkin, V., Balbashov, A. & Loidl, A. Possible  
233 evidence for electromagnons in multiferroic manganites. *Nature Physics.* **2**, 97-100 (2006),  
234 <http://www.nature.com/articles/nphys212>
- 235 [5] Rovillain, P., Cazayous, M., Gallais, Y., Measson, M., Sacuto, A., Sakata,  
236 H. & Mochizuki, M. Magnetic Field Induced Dehybridization of the Electro-  
237 magnons in Multiferroic TbMnO<sub>3</sub>. *Physical Review Letters.* **107**, 027202 (2011),  
238 <https://link.aps.org/doi/10.1103/PhysRevLett.107.027202>
- 239 [6] Sushkov, A., Aguilar, R., Park, S., Cheong, S. & Drew, H. Electromagnons in  
240 Multiferroic YMn<sub>2</sub>O<sub>5</sub> and TbMn<sub>2</sub>O<sub>5</sub>. *Physical Review Letters.* **98**, 027202 (2007),  
241 <https://link.aps.org/doi/10.1103/PhysRevLett.98.027202>
- 242 [7] Sushkov, A., Mostovoy, M., Valdés Aguilar, R., Cheong, S. & Drew, H. Electromagnons  
243 in multiferroic RMn<sub>2</sub>O<sub>5</sub> compounds and their microscopic origin. *Journal Of Physics:*  
244 *Condensed Matter.* **20**, 434210 (2008), [https://iopscience.iop.org/article/10.1088/0953-](https://iopscience.iop.org/article/10.1088/0953-8984/20/43/434210)  
245 [8984/20/43/434210](https://iopscience.iop.org/article/10.1088/0953-8984/20/43/434210)
- 246 [8] Stanislavchuk, T., Wang, Y., Janssen, Y., Carr, G., Cheong, S. & Sirenko, A. Magnon and  
247 electromagnon excitations in multiferroic DyFeO<sub>3</sub>. *Physical Review B.* **93**, 094403 (2016),  
248 <http://link.aps.org/doi/10.1103/PhysRevB.93.054113>
- 249 [9] Cazayous, M., Gallais, Y., Sacuto, A., Sousa, R., Lebeugle, D. & Colson, D. Possible Obser-  
250 vation of Cycloidal Electromagnons in BiFeO<sub>3</sub>. *Physical Review Letters.* **101**, 037601 (2008),  
251 <https://link.aps.org/doi/10.1103/PhysRevLett.101.037601>

- 252 [10] Rovillain, P., Cazayous, M., Gallais, Y., Sacuto, A., Lobo, R., Lebeugle, D. & Colson, D.  
253 Polar phonons and spin excitations coupling in multiferroic BiFeO<sub>3</sub> crystals. *Physical Review*  
254 *B.* **79**, 180411 (2009), <https://link.aps.org/doi/10.1103/PhysRevB.79.180411>
- 255 [11] Skiadopoulou, S., Goian, V., Kadlec, C., Kadlec, F., Bai, X., Infante, I., Dkhil, B., Adamo,  
256 C., Schlom, D. & Kamba, S. Spin and lattice excitations of a BiFeO<sub>3</sub> thin film and ceramics.  
257 *Physical Review B.* **91**, 174108 (2015), <https://link.aps.org/doi/10.1103/PhysRevB.91.174108>
- 258 [12] Lebeugle, D., Colson, D., Forget, A., Viret, M., Bonville, P., Marucco, J.  
259 & Fusil, S. Room-temperature coexistence of large electric polarization and mag-  
260 netic order in BiFeO<sub>3</sub> single crystals. *Physical Review B.* **76**, 024116 (2007),  
261 <http://link.aps.org/doi/10.1103/PhysRevB.76.024116>
- 262 [13] Sousa, R. & Moore, J. Electrical control of magnon propagation in multiferroic BiFeO<sub>3</sub> films.  
263 *Applied Physics Letters.* **92**, 022514 (2008), <http://aip.scitation.org/doi/10.1063/1.2835704>
- 264 [14] Chang, C., Mani, B., Lisenkov, S. & Ponomareva, I. Prediction of electromagnons in antifer-  
265 romagnetic ferroelectrics from first-principles: The case of BiFeO<sub>3</sub>. *Ferroelectrics.* **494**, 68-75  
266 (2016), <http://www.tandfonline.com/doi/abs/10.1080/00150193.2016.1137470>
- 267 [15] Seki, S., Kida, N., Kumakura, S., Shimano, R. & Tokura, Y. Electromagnons in the Spin  
268 Collinear State of a Triangular Lattice Antiferromagnet. *Physical Review Letters.* **105**, 097207  
269 (2010), <https://link.aps.org/doi/10.1103/PhysRevLett.105.097207>
- 270 [16] Chen, H., Li, Y. & Berakdar, J. Electric-field control of electromagnon propagation and spin-  
271 wave injection in a spiral multiferroic/ferromagnet composite. *Journal Of Applied Physics.*  
272 **117** (2015), <http://dx.doi.org/10.1063/1.4906520>
- 273 [17] Davydova, M., Zvezdin, K., Mukhin, A. & Zvezdin, A. Spin dynamics, antiferrodistortion and  
274 magnetoelectric interaction in multiferroics. The case of BiFeO<sub>3</sub>. *Physical Sciences Reviews.*  
275 **5**, 1-15 (2020), <https://www.degruyter.com/document/doi/10.1515/psr-2019-0070/html>
- 276 [18] Sayedaghaee, S., Prosandeev, S., Prokhorenko, S., Nahas, Y., Paillard, C., Xu, B. & Bellaiche,  
277 L. Domain-wall-induced electromagnons in multiferroics. *Physical Review Materials.* **6**, 034403  
278 (2022), <https://link.aps.org/doi/10.1103/PhysRevMaterials.6.034403>
- 279 [19] Sayedaghaee, S., Xu, B., Prosandeev, S., Paillard, C. & Bellaiche, L. Novel dynamical mag-  
280 netoelectric effects in multiferroic BiFeO<sub>3</sub>. *Physical Review Letters.* **122**, 097601 (2019)
- 281 [20] Sayedaghaee, S., Paillard, C., Prosandeev, S., Xu, B. & Bellaiche, L. Strain-induced resonances  
282 in the dynamical quadratic magnetoelectric response of multiferroics. *Npj Computational Ma-*

- 283 *terials*. **6**, 1-6 (2020)
- 284 [21] Stenberg, M. & Sousa, R. Model for twin electromagnons and magnetically induced os-  
285 cillatory polarization in multiferroic  $RMnO_3$ . *Physical Review B*. **80**, 094419 (2009),  
286 <https://link.aps.org/doi/10.1103/PhysRevB.80.094419>
- 287 [22] Lachheb, M., Zhu, Q., Fusil, S., Wu, Q., Carrétéro, C., Vecchiola, A., Bibes, M.,  
288 Martinotti, D., Mathieu, C., Lubin, C., Pancotti, A., Li-Bourrelier, X., Gloter, A.,  
289 Dkhil, B., Garcia, V. & Barrett, N. Surface and bulk ferroelectric phase transition  
290 in super-tetragonal  $BiFeO_3$  thin films. *Physical Review Materials*. **5**, 024410 (2021),  
291 <https://doi.org/10.1103/PhysRevMaterials.5.024410>
- 292 [23] Cherifi, S., Hertel, R., Fusil, S., Béa, H., Bouzehouane, K., Allibe, J., Bibes, M. & Barthélémy,  
293 A. Imaging ferroelectric domains in multiferroics using a low-energy electron microscope in  
294 the mirror operation mode. *Physica Status Solidi (RRL) - Rapid Research Letters*. **4**, 22-24  
295 (2010,2), <https://onlinelibrary.wiley.com/doi/10.1002/pssr.200903297>
- 296 [24] Gruverman, A., Alexe, M. & Meier, D. Piezoresponse force microscopy and nanoferroic phe-  
297 nomena. *Nature Communications*. **10**, 1661 (2019), [http://dx.doi.org/10.1038/s41467-019-](http://dx.doi.org/10.1038/s41467-019-09650-8)  
298 [09650-8](http://dx.doi.org/10.1038/s41467-019-09650-8)
- 299 [25] Kholkin, A., Kalinin, S., Roelofs, A. & Gruverman, A. Review of Ferroelectric Domain Imaging  
300 by Piezoresponse Force Microscopy. *Scanning Probe Microscopy*. **2** pp. 173-214 (2007)
- 301 [26] Prosandeev, S., Wang, D., Ren, W., Íñiguez, J. & Bellaiche, L. Novel nanoscale twinned phases  
302 in perovskite oxides. *Advanced Functional Materials*. **23**, 234-240 (2013)
- 303 [27] Prosandeev, S., Yang, Y., Paillard, C. & Bellaiche, L. Displacement current in domain walls  
304 of bismuth ferrite. *Npj Computational Materials*. **4**, 1-9 (2018)
- 305 [28] Wang, D., Weerasinghe, J. & Bellaiche, L. Atomistic molecular dynamic simulations of mul-  
306 tiferroics. *Physical Review Letters*. **109**, 067203 (2012)
- 307 [29] García-Palacios, J. & Lázaro, F. Langevin-dynamics study of the dynamical properties of  
308 small magnetic particles. *Physical Review B*. **58**, 14937 (1998)
- 309 [30] Hlinka, J., Paściak, M., Körbel, S. & Marton, P. Terahertz-range polar modes in domain-  
310 engineered  $BiFeO_3$ . *Physical Review Letters*. **119**, 057604 (2017)
- 311 [31] Xu, B., Íñiguez, J. & Bellaiche, L. Designing lead-free antiferroelectrics for energy storage.  
312 *Nature Communications*. **8**, 1-8 (2017)

- 313 [32] Boyn, S., Grollier, J., Lecerf, G., Xu, B., Locatelli, N., Fusil, S., Girod, S., Carrétéro, C.,  
314 Garcia, K., Xavier, S., Tomas, J., Bellaiche, L., Bibes, M., Barthélémy, A., Saïghi, S. &  
315 Garcia, V. Learning through ferroelectric domain dynamics in solid-state synapses. *Nature*  
316 *Communications*. **8**, 14736 (2017), <http://www.nature.com/articles/ncomms14736>
- 317 [33] Rovillain, P., De Sousa, R., Gallais, Y., Sacuto, A., Méasson, M., Colson, D., Forget, A., Bibes,  
318 M., Barthélémy, A. & Cazayous, M. Electric-field control of spin waves at room temperature  
319 in multiferroic BiFeO<sub>3</sub>. *Nature Materials*. **9**, 975-979 (2010)
- 320 [34] Cazayous, M., Malka, D., Lebeugle, D. & Colson, D. Electric field effect on Bi Fe O 3 single  
321 crystal investigated by Raman spectroscopy. *Applied Physics Letters*. **91**, 071910 (2007)
- 322 [35] Lobo, R., Moreira, R., Lebeugle, D. & Colson, D. Infrared phonon dynamics of a multiferroic  
323 BiFeO<sub>3</sub> single crystal. *Physical Review B*. **76**, 172105 (2007)
- 324 [36] Haumont, R., Kreisel, J., Bouvier, P. & Hippert, F. Phonon anomalies and the ferroelectric  
325 phase transition in multiferroic BiFeO<sub>3</sub>. *Physical Review B*. **73**, 132101 (2006)
- 326 [37] Kamba, S., Nuzhnyy, D., Savinov, M., Šebek, J., Petzelt, J., Prokleška, J., Haumont, R. &  
327 Kreisel, J. Infrared and terahertz studies of polar phonons and magnetodielectric effect in  
328 multiferroic BiFeO<sub>3</sub> ceramics. *Physical Review B*. **75**, 024403 (2007)

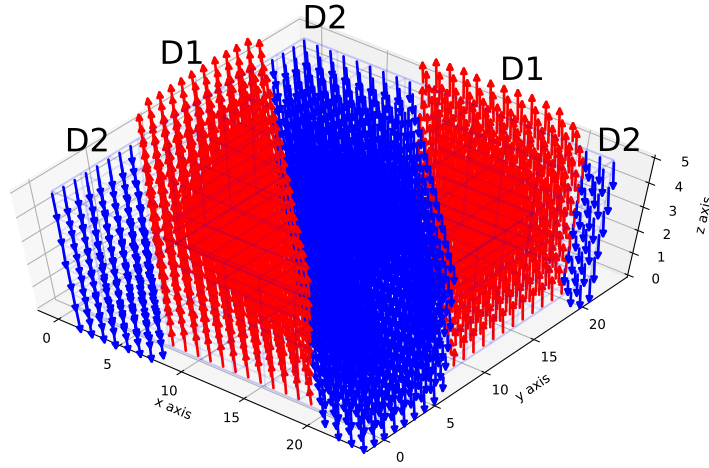


FIG. 1: (Color online) Schematic representation of the zero-field electric dipole moments' pattern for our studied  $24 \times 24 \times 6$  supercell of  $\text{BiFeO}_3$ . The blue and red vectors are used to represent electric dipole moments along the  $[1\bar{1}\bar{1}]$  and  $[\bar{1}11]$  directions, respectively.

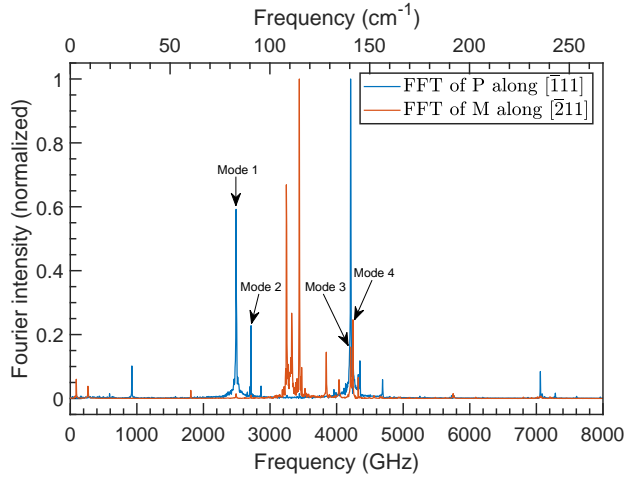


FIG. 2: (Color online) Fourier analyses of polarization and magnetization. The frequency spectrum of the component of electrical dipole moments along the  $[\bar{1}11]$  direction (blue) and magnetic moments along the  $[211]$  direction (orange) obtained by Fourier analysis when the applied  $dc$  electric field is  $1 \times 10^7 V/m$ . The frequency of the modes shown by black arrows significantly shifts upon applying different magnitudes of electric field.

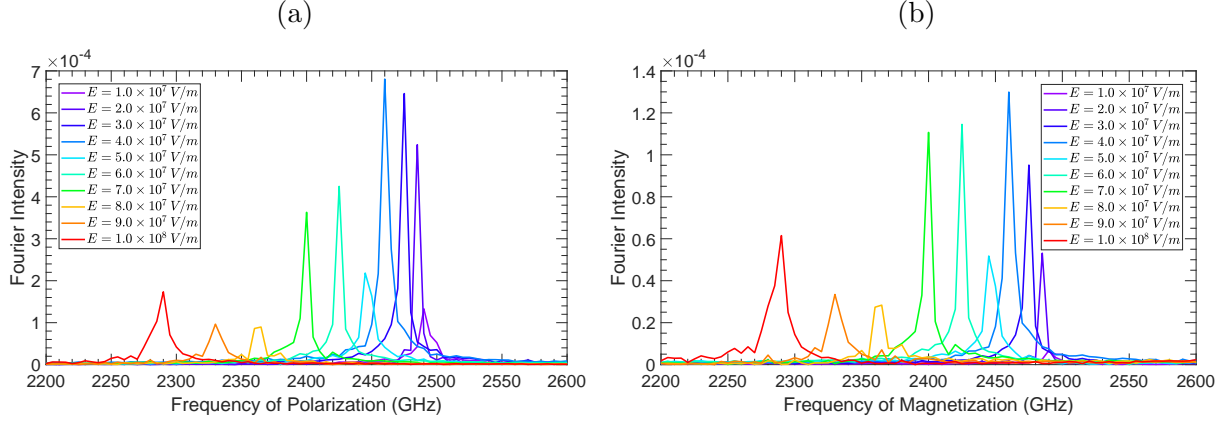


FIG. 3: (Color online) Frequency shift of optical phonons and magnons of Mode 1. (a) The shift of the frequency observed for the optical phonons upon the application of various  $dc$  electric fields. (b) The shift of the frequency observed for the magnons upon the application of various  $dc$  electric fields. For both cases the applied electric field changes from  $1.0 \times 10^7$  V/m to  $1.0 \times 10^8$  V/m.



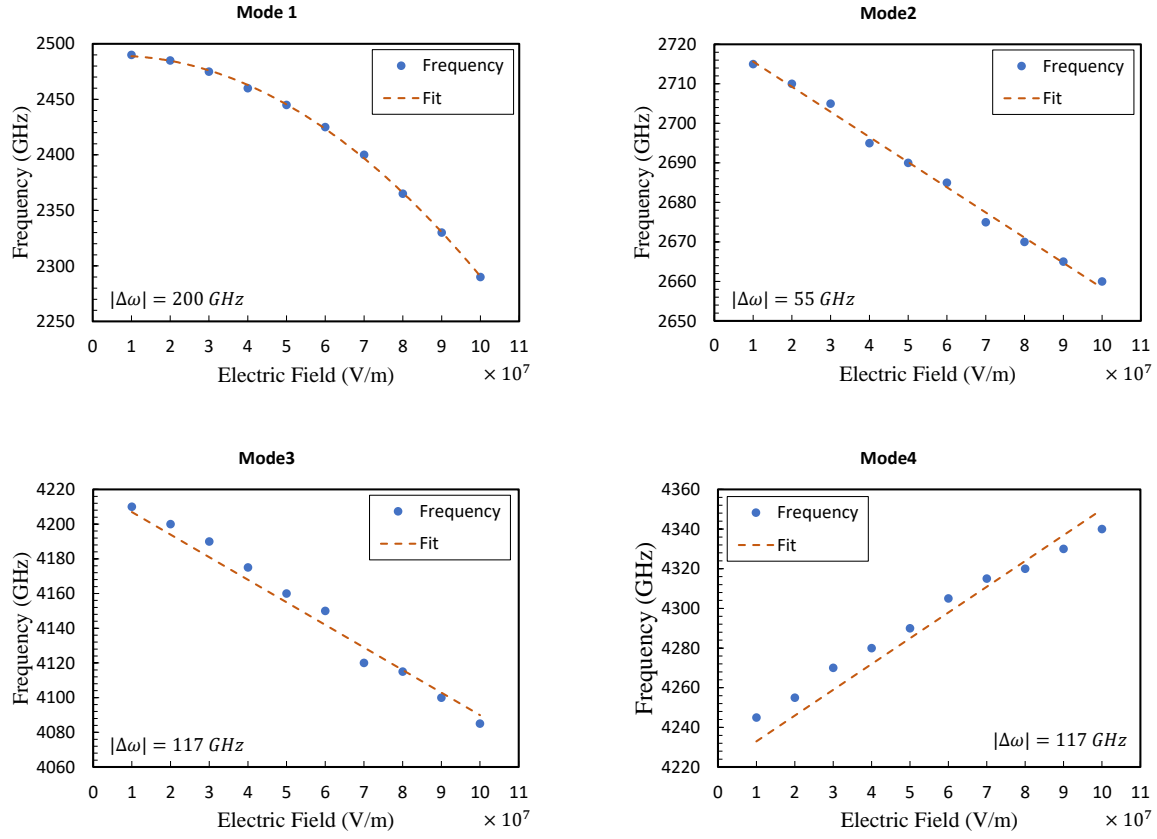


FIG. 4: (Color online) Frequency shift of four electromagnons. In each panel, the frequency shift of the corresponding mode *versus* the applied electric fields is shown. A polynomial fit of second order for Mode 1, and of first order for Modes 2, 3, and 4 is applied.  $|\Delta\omega|$  is the magnitude of the difference between the highest and the lowest frequencies of the fitted lines for our chosen range of applied electric fields.

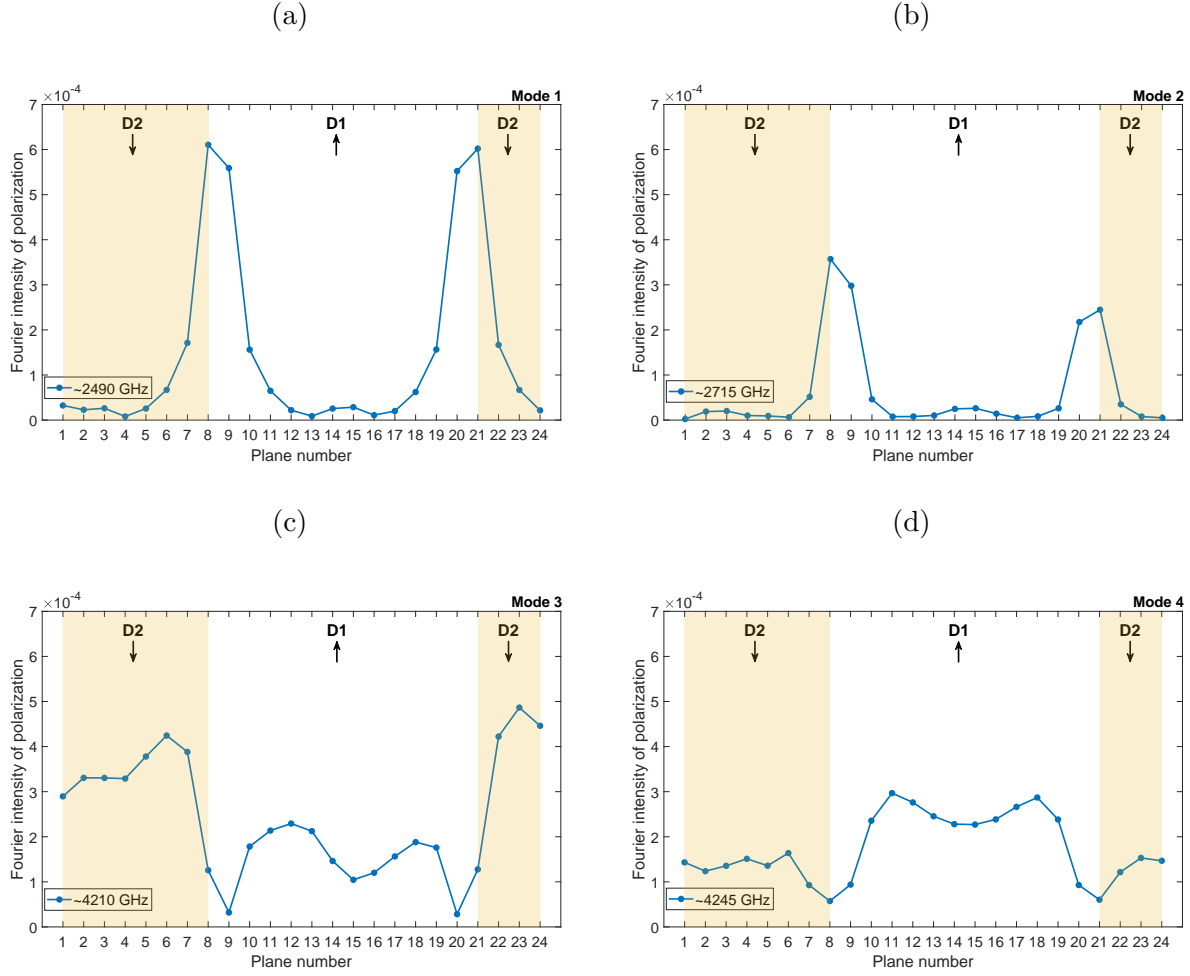


FIG. 5: (Color online) The degree of localization of the electromagnons possessing significant frequency shift under the application of electric fields. In each panel, the degree of localization of the corresponding mode at the planes parallel to the domain walls within the investigated supercell is shown. The shaded area corresponds to the domains possessing electric dipoles pointing along the  $[\bar{1}\bar{1}\bar{1}]$  direction, while the white area corresponds to the domains possessing electric dipoles pointing along the opposite  $[\bar{1}11]$  direction. The arrow in each domain indicates the direction of the z-component of electric dipole moments present in the domain. The applied electric field for all cases is  $E = 1.0 \times 10^7 V/m$  along the  $[\bar{1}11]$  direction which is parallel to the direction of the electric dipoles in D1 and antiparallel to the direction of the electric dipoles in D2.